Kinetik: Game Technology, Information System, Computer Network, Computing, Electronics, and Control
Journal homepage: http://kinetik.umm.ac.id
ISSN: 2503-2267
Vol. 10, No. 1, February, Pp. 29-36

Detecting acute lymphoblastic leukemia in blood smear images using CNN and SVM

Nelly Oktavia Adiwijaya*[,1], Sultan Ardiansyah[1], Dwiretno Istiyadi Swasono[1]
Faculty of Computer Science, University of Jember, Jember, Indonesia[1]

Article Info
Keywords:
Convolutional Neural Network, Support Vector Machine, EfficientNet, Peripheral Blood Smear Image, Acute Lymphoblastic Leukemia

Article history:
Received: May 29, 2024
Accepted: December 06, 2024
Published: February 01, 2025

Cite:
N. O. Adiwijaya, S. Ardiansyah, and D. I. . Swasono, "Detecting Acute Lymphoblastic Leukemia in Blood Smear Images using CNN and SVM", *KINETIK*, vol. 10, no. 1, Feb. 2025.
https://doi.org/10.22219/kinetik.v10i1.2027

*Corresponding author.
Nelly Oktavia Adiwijaya
E-mail address:
nelly.oa@unej.ac.id

Abstract
Acute Lymphoblastic Leukemia (ALL) is a common and aggressive subtype of leukemia that predominantly affects children. Accurate and timely diagnosis of ALL is critical for successful treatment, but it is hindered by the limitations of manual examination of peripheral blood smear images, which are prone to human error and inefficiency. This study proposes an improved diagnostic approach by integrating the EfficientNet architecture with a Support Vector Machine (SVM) classifier to enhance classification accuracy and address the performance inconsistencies of standalone EfficientNet models. Additionally, a novel CNN-based model with a reduced number of parameters is developed and evaluated. A dataset comprising 3.256 peripheral blood smear images across four classes (benign, early, pre and pro) was used for training and testing. The EfficientNet-SVM models achieved a peak accuracy of 97.35% using the EfficientNet-B3 architecture, surpassing previous studies. The improved CNN model achieved the highest accuracy of 99.18% while reducing parameters by 59.5% compared to the best prior models, with a negligible accuracy decrease of only 0.67%. These findings highlight the potential of combining EfficientNet with SVM and the efficiency of the improved CNN model for automated ALL detection, paving the way for more reliable, cost-effective, and scalable diagnostic tools.

1. Introduction

Blood cancer is one of the most dangerous diseases in humans. As the name implies, this cancer attacks blood cells in humans by changing or mutating blood cells so that the blood cells become abnormal. One of the most common types of blood cancer is leukemia. Leukemia is a blood cancer that attacks white blood cells in the bone marrow so that the white blood cells become abnormal and cause the body's immune system to decrease [1][2]. From 2003 to 2007, there were 717,863 cases of leukemia occurring in 185 countries. Meanwhile, in 2012 new cases of leukemia were found with an estimated number of 350,000 cases. By 2018, the highest cases of leukemia occurred in Australia and New Zealand (with age-standardized rate per 100,000 cases of 11.3 in men and 7.2 in women), North America (with age-standardized rate per 100,000 cases of 10 .5 in men and 7.2 in women), and continental western Europe (with age-standardized rate per 100,000 cases of 9.6 in men and 6.0 in women). The lowest cases of leukemia occurred in West Africa (with age-standardized rate per 100,000 cases of 1.4 in men and 1.2 in women) [3].

Among the various subtypes of leukemia, acute lymphoblastic leukemia (ALL) is a type of leukemia blood cancer with the highest cases affecting children in various countries [1] [4]. Leukemia is more dominant in children aged under 15 years with cases per year reaching 3 to 4 cases per 100,000 children. In addition, leukemia is more common in boys than girls. Currently, the standard method for diagnosing ALL involves manual examination of peripheral blood smear samples under a microscope by trained experts [5]. While this approach is effective, it is labor-intensive, time-consuming, and prone to errors due to fatigue and subjective judgement, especially when dealing with large numbers of samples [4][6].

To address these limitations, computerized approaches that leverage machine learning (ML) and deep learning (DL) gave gained traction [1][7][8]. These techniques allow for automated detection, classification, and analysis of blood smear images, significantly reducing reliance on manual expertise and improving diagnostic efficiency [5][9][10]. Among the DL methods, Convolutional Neural Networks (CNNs) have demonstrated superior performance in image processing tasks due to their ability to automatically learn features from images through layered structures, including input, hidden, and output layers [8][10][11][12][13][14]. Studies using CNN architectures such as MobileNetV2, ResNet18, and VGG16 have achieved remarkable accuracy in ALL classification, ranging from 97% to 99.39% [1][5].

However, despite these advancement, challenges remain [15]. One notable issues is the inconsistent performance of certain CNN architectures, such as EfficientNet, which, while theoretically superior, produces unexpectedly low accuracy (28.22%) in ALL classification tasks, as reported by [16][17]. This contradiction highlights the need for further research to optimize and adapt CNN architectures to the specific requirements of blood smear

image analysis. Additionally, support vector machines (SVMs) have proven effective in maximizing classification accuracy in ML, but their integration with modern CNN architectures remains underexplored in the context of ALL detection [18].

Given these gaps, this study aims to enhance the performance of EfficientNet for ALL classification by integrating it with SVM, leveraging SVM's robustness in classification tasks. By combining the strength of both approaches, this research seeks to develop a more reliable and accurate system for ALL detection. The proposed method will address existing challenges, including inconsistent performance and model optimization, to contribute to more effective diagnostic tools for healthcare practitioners.

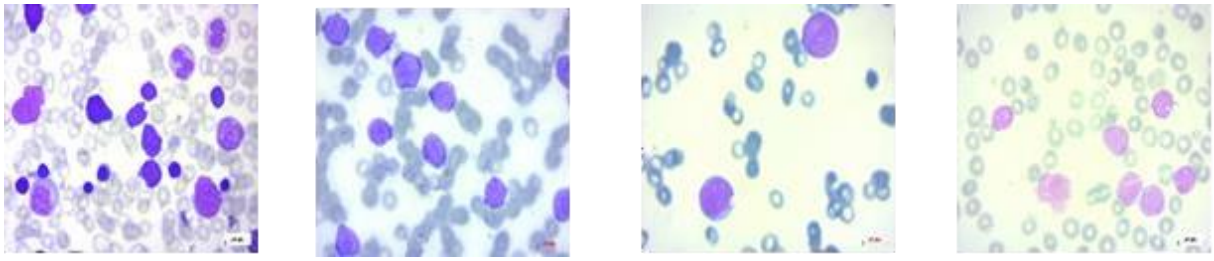

Figure 1. Acute Lymphoblastic Leukemia on Peripheral Blood Smear Image. In Order from Left to Right, the Classes are Benign, Early, Pre, Pro

2. Research Method

2.1 Dataset

The dataset used is the acute lymphoblastic leukemia disease dataset on the peripheral blood smear image. This dataset was obtained from a public source, namely the public dataset provider website www.kaggle.com with authors named Mehrad Aria, Mustafa Ghaderzadeh, Davood Bashash, Hassan Abolghasemi, Farkhondeh Asadi, and Azamossadat Hosseini [19]. This dataset was previously prepared in the bone marrow laboratory of Taleqani Hospital, Tehran. Data in the form of digital images of peripheral blood smears were observed microscopically with a magnification of 100x and photographed in JPG format as shown in Figure 1. The resolution of the image used is changed to a size of 224x224 or 128x128 pixels according to the architecture due to the limited specifications of the device used. Peripheral blood smear is a sample of broken blood cells with incomplete nuclear membranes without cytoplasm [20]. There are 3256 images in total and divided into 4 classes with a distribution of 504 benign class images, 985 early class images, 963 pre class images, and 804 pro class images [16]. In identifying the four classes of acute lymphoblastic leukemia, knowledge of the characteristics of each class is required. Table 1 shows the different features of acute lymphoblastic leukemia.

Table 1. Characteristics of Each Class of Acute Lymphoblastic Leukemia

Class	Characteristics
Benign	Small cells about 10 – 20 nanometers in diameter [21]
Early	Medium-sized lymphoblast cells are slightly indented and have large nucleoli [22]
Pre	Lymphoblast cells are small or large with a round nucleus [23] [24]
Pro	Lymphoblast cells that are still in the basophilic stage with several Nucleoli [25][26]

2.2 Model architecture

A model was designed to identify the shape of cells in acute lymphoblastic leukemia in peripheral blood smear images using two CNN models. The two models are EfficientNet with SVM and Improved model.

2.2.1 EfficientNet model with SVM

EfficientNet has 8 architectures, including EfficientNetB0, EfficientNetB1, EfficientNetB2, EfficientNetB3, EfficientNetB4, EfficientNetB5, EfficientNetB6, and EfficientNetB7 which are distinguished by the number of parameters. In this research, the EfficientNet architecture was able to outperform several other transfer learning architectures, such as ResNet50, DenseNet-169, InceptionV3, PolyNet, and several other architectures [17]. However, in a study aimed at diagnosing acute lymphoblastic leukemia in peripheral blood smear images using

EfficientNet, the accuracy was very low, so this needs to be improved. In this study, the EfficientNet model is combined with SVM. All eight EfficientNet architectures were used and combined with SVM.

EfficientNet architecture acted as feature extraction, while SVM acted as a feature classification model. EfficientNet architecture with SVM is depicted in Figure 2.

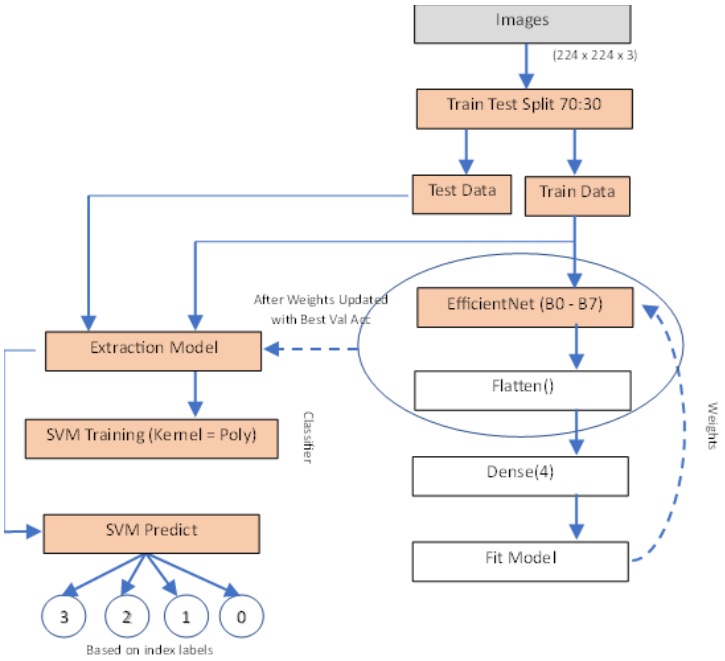

Figure 2. EfficientNet with SVM Architecture

2.2.2 Improved model

Improved model is a simple CNN model that is created manually by specifying several layers. The Improved Model architecture uses 5 types of layers, including Conv2D, MaxPooling2D, Flatten, Dense, and Dropout. Improved Model Architecture is taken from one study with a different research object [27]. According to the model architecture depicted in Figure 3, the peripheral blood smear image with a size of 224x224x3 passes through the Conv2D layer for convolution process with 32 filters, 3x3 kernel size and ReLU activation.

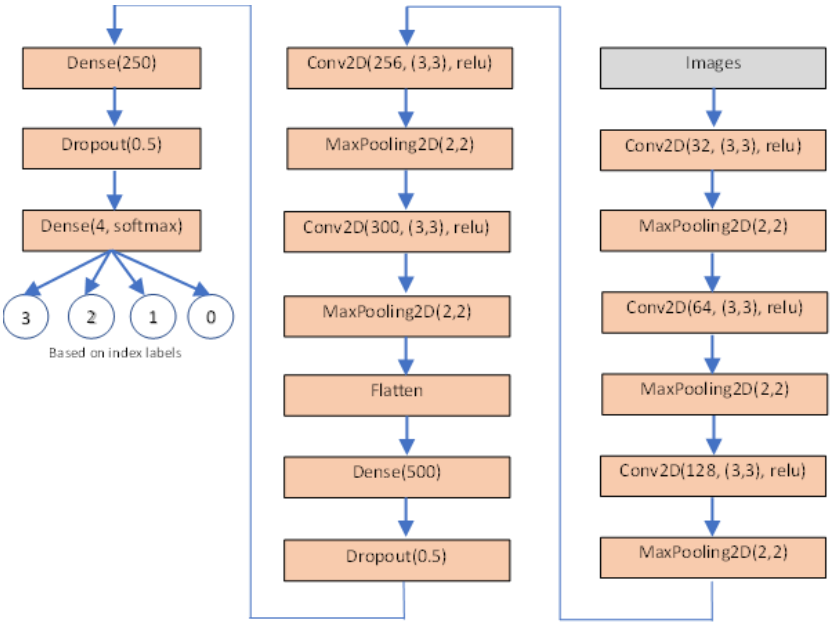

Figure 3. Improved Model Architecture

ReLU activation plays a role after the image goes through a convolution process to handle pixel values that are below 0 or negative and change it to 0. The output of this process is after passing through the Conv2D layer, the image will enter the MaxPooling2D layer with a pooling size parameter of 2x2. In this layer the convoluted image will undergo a process of eliminating pixels in the specified pooling area by finding the maximum value. After that, the output of the MaxPooling2D layer will be repeated 4 times using the Conv2D and MaxPooling2D layers with the same parameters. The output from the previous process then goes to the Flatten layer. In this layer the output image is converted into a 1- dimensional array. The array then goes to the Dense layer. This Dense layer is a Fully Connected layer that aims to process matrix multiplication. The Dense layer parameter used is 500 units. The output from the Dense layer then goes to the Dropout layer with a rate of 0.5. This Dense layer will randomly ignore neurons during model training to prevent overfitting. Furthermore, the output of the previous process is repeated to enter the Dense and Dropout layers, but in the next Dense layer, only 250 units of parameter is used. The output from that process then enters the Dense layer with 4 units of parameter and softmax activation. 4 units is used as the number of labels in the dataset, while softmax activation is used as an output classification for labels. The final result of this layer is the percentage probability of the predicted label being correct.

2.3 Model training and testing

The image used for the training model on the EfficientNetB0 to EfficientNetB5 architecture is 224x224 pixels, while the EfficientNetB6 and EfficientNetB7 architectures use 128x128 pixels. Furthermore, for the needs of training, testing and evaluation on each architecture, train-test split procedure is implemented on the dataset. The train-test split technique is used with the aim of dividing the data into training data and testing data. The training data is used to train the model and the testing data is used to validate and evaluate the previously trained model [28]. The image used for training models on all architectures is 224x224 pixels in size.

2.3.1 Model EfficientNet with SVM

In this study, the ratio of the train-test split of the dataset is 70% for the training data and 30% for the testing data. The train-test split method also uses the stratify parameter based on its class, aiming to divide equally for each class. The results obtained for the training and testing data are 2279 and 977 images respectively. Class labels are also converted into numbers by encoding process so that the model training can be conducted. The distribution of the dataset after passing through the solving process is shown in Table 2. Furthermore, the process of model training and testing is different for each model [29]. In the model testing process, the testing data goes through a feature extraction and feature classification process that has been trained so that it gets the output in the form of classification.

Table 2. Dataset Split Distribution

Class	Encode	Training data	Testing data
Benign	0	353	151
Early	1	689	296
Pre	2	674	289
Pro	3	563	241
Total		2279	977

2.3.2 Improved model

The training data that has been prepared previously is directly used in the training process on the improved model architecture. The training model process on the improved model architecture is carried out by adding a validation split parameter of 10% so that the training model validation accuracy can be monitored. In addition, the repetition of training or epochs used is 500 epochs. The best percentage of validation accuracy in an epoch is the training model used. In the model testing process, the testing data is directly tested using a model that has been trained previously so that it gets the output in the form of classification.

2.4 Evaluation

The two models that have been previously trained and tested are then evaluated by calculating the accuracy of each model architecture so that the accuracy value of the models created can be obtained [30]. The test result data or prediction data is compared with the testing data to obtain the accuracy value (acc = prediction label data/test label data * 100%).

3. Results and Discussion

3.1 Results

The research was conducted using 2 types of models, namely the EfficientNet model with SVM and the improved model. The EfficientNet model with SVM used 7 types of architecture, including EfficientNetB0 with SVM, EfficientNetB1

with SVM, EfficientNetB2 with SVM, EfficientNetB3 with SVM, EfficientNetB4 with SVM, EfficientNetB5 with SVM, EfficientNetB6 with SVM, and EfficientNetB7 with SVM. The EfficientNet architecture has improved better accuracy results after being combined with SVM when compared to other studies that used the EfficientNet architecture and used a dataset of 4 classes. While the improved model architecture obtained high accuracy with quite a few parameters. The results of the accuracy test on the EfficientNet model with SVM and the improved model are shown in Table 3.

Table 3. Comparison of EfficientNet Model with SVM and EfficientNet model

Architecture	Accuracy	Resolution	Parameter
EfficientNetB0 with SVM	83,93%	224x224	4 M
EfficientNetB1 with SVM	54,88%	224x224	6,5 M
EfficientNetB2 with SVM	74,64%	224x224	7,7 M
EfficientNetB3 with SVM	97,35%	224x224	10,7 M
EfficientNetB4 with SVM	86,04%	224x224	17,6 M
EfficientNetB5 with SVM	95,3%	224x224	28,5 M
EfficientNetB6 with SVM	45,67%	128x128	40,9 M
EfficientNetB7 with SVM	38,29%	128x128	64 M
Improved Model	**99,18%**	224x224	**8,1 M**

It can be seen from Table 3 that in identifying acute lymphoblastic leukemia in peripheral blood smear images, tthe model obtaining the highest accuracy was EfficientNetB4 architecture with SVM. As for the overall architectures, the highest accuracy value was found in the improved model architecture. The EfficientNet model with SVM in this study is a development of a research conducted by Ghaderzadeh et al. which used EfficientNet model, while the improved model applied the architectural model of the research conducted by Asma Maqsood et al. The EfficientNet architecture has obtained higher accuracy after being combined with SVM in comparison to other studies that used EfficientNet architecture and a dataset of 4 classes. Meanwhile, the architecture of the improved model obtains accuracy results that outperform most of the models in Ghaderzadeh's study.

3.2 Discussion

The results obtained from this study indicate that acute lymphoblastic leukemia can be identified on the peripheral blood smear using CNN and SVM methods. This study resulted in 2 models, namely the EfficientNet model with SVM and the Improved model. In the first model, EfficientNet is used as an image feature extractor while SVM is used as an object classification. EfficientNet has 8 architectural variations which were all used in this study, including EfficientNetB0, EfficientNetB1, EfficientNetB2, EfficientNetB3, EfficientNetB4, EfficientNetB5, EfficientNetB6, and EfficientNetB7. This model shows an increase in accuracy results compared to the previous study conducted by Ghaderzadeh, et al., where the study resulted in an accuracy of 28.22%. Research conducted by Ghaderzadeh, et al., and this study used a dataset of acute lymphoblastic leukemia on peripheral blood smear images with 4 classes, namely benign, early, pre class, and pro. Table 4 shows the comparison of the accuracy results in this study with those of Ghaderzadeh et al.

Table 4. Comparison of the Model in this Study with Research by Ghaderzadeh et al

Research	Architecture	Accuracy	Resolution	Parameter
This study	EfficientNetB0 with SVM	83,93%	224x224	4 M
	EfficientNetB1 with SVM	54,88%	224x224	6,5 M
	EfficientNetB2 with SVM	74,64%	224x224	7,7 M
	EfficientNetB3 with SVM	97,35%	224x224	10,7 M
	EfficientNetB4 with SVM	86,04%	224x224	17,6 M
	EfficientNetB5 with SVM	95,3%	224x224	28,5 M
	EfficientNetB6 with SVM	45,67%	128x128	40,9 M
	EfficientNetB7 with SVM	38,29%	128x128	64 M
	Improved model	99,18%	224x224	8,1 M
[16]	EfficientNet	28,22%	224x224	4 M [17]
	MobileNetV3	50.15%	224x224	5,3 M [31]
	VGG-19	96.32%	224x224	144 M [32]
	Xception	96.70%	224x224	22,8 M [33]
	InceptionV3	96.93%	224x224	25 M [34]
	ResNet50V2	97.85%	224x224	4,6 M [35]

VGG-16	98.01%	224x224	138 M [32]
NASNetLarge	98.16%	224x224	27,6 M [36]
InceptionResNetV2	99.54%	224x224	133 M [37]
DenseNet201	99.85%	224x224	20 M [38]

The increase was due to the role of SVM in this study. The accuracy obtained from all EfficientNet models, , namely EfficientNetB0, EfficientNetB1, EfficientNetB2, EfficientNetB3, EfficientNetB4, EfficientNetB5, EfficientNetB6, and EfficientNetB7, combined with SVM were 83.93%, 54.88%, 74.64%, 97.35%, 86.04%, 95.3%, 45.67%, and 38.29% respectively. From each of these architectures, the highest accuracy result was obtained from the EfficientNetB3 architecture, which is 97.35%.

Improved model in this study obtained an accuracy of 99.18%. These results outperformed most of the models in the Ghaderzadeh's study and almost equaled the two models, namely InceptionResNetV2 and DenseNet101. The improved model had only 8.1 million parameters, but InceptionResNetV2 and DenseNet101 had much more parameters about 133 million and 20 million respectively. The improved model reduced the number of parameters by about 59.5% less than the best model in the previous study, with a decrease in accuracy of only 0.67%. The reduced number of parameters in the improved CNN model was achieved by simplifying its architecture while maintaining critical features essential for classification. By employing fewer layers and carefully selecting operations such as smaller convolutional filters, efficient pooling strategies, and dropout layers, the model minimizes computational overhead. The design also focuses on removing redundant features and emphasizing the most significant ones, resulting in optimized parameter usage. This streamlined approach avoids overfitting, as evidenced by the slight decrease in accuracy (0.67%) compared to models with higher parameter counts like DenseNet101, while achieving significant resource efficiency.

4. Conclusion

This research aimed to improve the classification accuracy of Acute Lymphoblastic Leukemia (ALL) detection from peripheral blood smear images by integrating the EfficientNet architecture with a Support Vector Machine (SVM) classifier and developing an improved CNN model with fewer parameters. The proposed models address the challenges of performance inconsistencies in existing EfficientNet models and the need for resource-efficient architectures.

The EfficientNet-SVM combination demonstrated significant improvements, achieving a peak accuracy of 97.35% using the EfficientNet-B3 architecture, which outperformed similar models in prior studies. Furthermore, the improved CNN model achieved the highest accuracy of 99.18%, with a substantial 59.5% reduction in parameters compared to state-of-the-art models, demonstrating its computational efficiency and practical applicability. The streamlined design of the improved CNN model effectively balanced parameter optimization and high classification accuracy, making it suitable for deployment in resource-constrained environments.

These findings imply that integrating EfficientNet with SVM can enhance feature classification, while architectural refinements in CNN models can reduce computational demands without compromising the performance. Future research should explore deploying these models in real-world clinical settings and enhancing generalizability across diverse datasets to further validate and extend their applicability.

Acknowledgement

The authors would like to thank Department of Computer Science, Universitas Jember, Indonesia for the support during the implementation and research writing.

References

[1] P. K. Das and S. Meher, "An efficient deep Convolutional Neural Network based detection and classification of Acute Lymphoblastic Leukemia," *Expert Syst Appl*, vol. 183, no. April, p. 115311, 2021. https://doi.org/10.1016/j.eswa.2021.115311

[2] R. Rompies, S. P. Amelia, and S. Gunawan, "Perubahan Status Gizi pada Anak dengan Leukemia Limfoblastik Akut Selama Terapi," *e-CliniC*, vol. 8, no. 1, pp. 152–157, 2019. https://doi.org/10.35790/ecl.8.1.2020.28290

[3] A. Miranda-Filho, M. Piñeros, J. Ferlay, I. Soerjomataram, A. Monnereau, and F. Bray, "Epidemiological patterns of leukaemia in 184 countries: a population-based study," *Lancet Haematol*, vol. 5, no. 1, pp. e14–e24, 2018. https://doi.org/10.1016/s2352-3026(17)30232-6

[4] K. Dese *et al.*, "Accurate Machine-Learning-Based classification of Leukemia from Blood Smear Images," *Clin Lymphoma Myeloma Leuk*, vol. 21, no. 11, pp. e903–e914, 2021. https://doi.org/10.1016/j.clml.2021.06.025

[5] A. Abhishek, R. K. Jha, R. Sinha, and K. Jha, "Automated classification of acute leukemia on a heterogeneous dataset using machine learning and deep learning techniques," *Biomed Signal Process Control*, vol. 72, no. PB, p. 103341, 2022. https://doi.org/10.1016/j.bspc.2021.103341

[6] C. C. Chang *et al.*, "Clinical significance of smudge cells in peripheral blood smears in hematological malignancies and other diseases," *Asian Pacific Journal of Cancer Prevention*, vol. 17, no. 4, pp. 1847–1850, 2016. https://doi.org/10.7314/apjcp.2016.17.4.1847

[7] R. Sarki, K. Ahmed, H. Wang, Y. Zhang, and K. Wang, "Automated detection of COVID-19 through convolutional neural network using chest x-ray images," *PLoS One*, vol. 17, no. 1 January, pp. 1–26, 2022. https://doi.org/10.1371/journal.pone.0262052

[8] C. Janiesch, P. Zschech, and K. Heinrich, "Machine learning and deep learning," *Electronic Markets*, vol. 31, no. 3, pp. 685–695, 2021. https://doi.org/10.1007/s12525-021-00475-2

[9] K. He, X. Zhang, S. Ren, and J. Sun, "Deep residual learning for image recognition," *Proceedings of the IEEE Computer Society Conference on Computer Vision and Pattern Recognition*, vol. 2016-Decem, pp. 770–778, 2016. https://doi.org/10.1109/CVPR.2016.90

[10] A. Krizhevsky, I. Sutskever, and G. E. Hinton, "ImageNet classification with deep convolutional neural networks," *Commun ACM*, vol. 60, no. 6, pp. 84–90, 2017. https://doi.org/10.1145/3065386
[11] G. Marques, D. Agarwal, and I. de la Torre Díez, "Automated medical diagnosis of COVID-19 through EfficientNet convolutional neural network," *Applied Soft Computing Journal*, vol. 96, p. 106691, 2020. https://doi.org/10.1016/j.asoc.2020.106691
[12] K. O'Shea and R. Nash, "An Introduction to Convolutional Neural Networks," Nov. 2015. https://doi.org/10.48550/arXiv.1511.08458
[13] Y. LeCun, L. Bottou, Y. Bengio, and P. Haffner, "Gradient-based learning applied to document recognition," *Proceedings of the IEEE*, vol. 86, no. 11, pp. 2278–2323, 1998. https://doi.org/10.1109/5.726791
[14] C. Szegedy *et al.*, "Going deeper with convolutions," *Proceedings of the IEEE Computer Society Conference on Computer Vision and Pattern Recognition*, vol. 07-12-June, pp. 1–9, 2015. https://doi.org/10.1109/CVPR.2015.7298594
[15] V. T. Hoang and K. H. Jo, "Slice Operator for Efficient Convolutional Neural Network Architecture," *Lecture Notes in Computer Science (including subseries Lecture Notes in Artificial Intelligence and Lecture Notes in Bioinformatics)*, vol. 12034 LNAI, no. March, pp. 163–173, 2020. https://doi.org/10.1007/978-3-030-42058-1_14
[16] M. Ghaderzadeh, M. Aria, A. Hosseini, F. Asadi, D. Bashash, and H. Abolghasemi, "A fast and efficient CNN model for B-ALL diagnosis and its subtypes classification using peripheral blood smear images," *International Journal of Intelligent Systems*, vol. 37, no. 8, pp. 5113–5133, 2022. https://doi.org/10.1002/int.22753
[17] M. Tan and Q. V. Le, "EfficientNet: Rethinking model scaling for convolutional neural networks," *36th International Conference on Machine Learning, ICML 2019*, vol. 2019-June, pp. 10691–10700, 2019. https://doi.org/10.48550/arXiv.1905.11946
[18] M. Mohammed, M. B. Khan, and E. B. M. Bashie, *Machine learning: Algorithms and applications*. CRC Press, 2016. https://doi.org/10.1201/9781315371658
[19] M. Aria, M. Ghaderzadeh, D. Bashash, H. Abolghasemi, F. Asadi, and A. Hosseini, "Acute Lymphoblastic Leukemia (ALL) image dataset," Kaggle. https://doi.org/10.1002/int.22753
[20] A. Sall *et al.*, "Smudge cells percentage on blood smear is a reliable prognostic marker in chronic lymphocytic leukemia," *Hematol Transfus Cell Ther*, vol. 44, no. 1, pp. 63–69, 2022. https://doi.org/10.1016/j.htct.2021.04.002
[21] S. P. Chantepie, E. Cornet, V. Salaün, and O. Reman, "Hematogones: An overview," Nov. 2013. https://doi.org/10.1016/j.leukres.2013.07.024
[22] B. Y. A. W. Harris, C. A. Pinkert, M. Crawford, W. Y. Langdon, R. L. Brinster, and J. M. Adams, "THE Et . -myc TRANSGENIC MOUSE A Model for High-incidence Spontaneous Lymphoma and Leukemia of Early B Cells Translocation of the c-myc protooncogene into or near one of the Ig loci is found in almost every case of Burkitt ' s B cell lymphoma in man and e," vol. 167, no. February, 1988.
[23] J. H. Cho-Vega, L. J. Medeiros, V. G. Prieto, and F. Vega, "Leukemia cutis," *Am J Clin Pathol*, vol. 129, no. 1, pp. 130–142, 2008. https://doi.org/10.1309/WYACYWF6NGM3WBRT
[24] F. E. Bertrand, C. Vogtenhuber, N. Shah, and T. W. Lebien, "Pro-B-cell to pre-B-cell development in B-lineage acute lymphoblastic leukemia expressing the MLL/AF4 fusion protein," *Blood*, vol. 98, no. 12, pp. 3398–3405, 2001. https://doi.org/10.1182/blood.v98.12.3398
[25] M. Urashima *et al.*, "Establishment of a Human pro-B Cell Line (JKB-1) and Its Differentiation of Preestablished Bone Marrow Stromal Cell Layer," 1994.
[26] M. Perez-Andres *et al.*, "Human peripheral blood B-Cell compartments: A crossroad in B-cell traffic," *Cytometry B Clin Cytom*, vol. 78, no. SUPPL. 1, pp. 47–60, 2010. https://doi.org/10.1002/cyto.b.20547
[27] A. Maqsood, M. S. Farid, M. H. Khan, and M. Grzegorzek, "Deep malaria parasite detection in thin blood smear microscopic images," *Applied Sciences (Switzerland)*, vol. 11, no. 5, pp. 1–19, 2021. https://doi.org/10.3390/app11052284
[28] V. Singh, M. Pencina, A. J. Einstein, J. X. Liang, D. S. Berman, and P. Slomka, "Impact of train/test sample regimen on performance estimate stability of machine learning in cardiovascular imaging," *Sci Rep*, vol. 11, no. 1, pp. 1–8, 2021. https://doi.org/10.1038/s41598-021-93651-5
[29] S. H. Abdulhussain, B. M. Mahmmod, M. A. Naser, M. Q. Alsabah, R. Ali, and S. A. R. Al-Haddad, "A robust handwritten numeral recognition using hybrid orthogonal polynomials and moments," *Sensors*, vol. 21, no. 6, pp. 1–18, 2021. https://doi.org/10.3390/s21061999
[30] E. F. Saraswita, "Akurasi Klasifikasi Citra Digital Scenes RGB Menggunakan Model K-Nearest Neighbor dan Naive Bayes," *Prosiding Annual Research Seminar*, vol. 5, no. 1, pp. 978–979, 2019.
[31] A. Howard *et al.*, "Searching for mobileNetV3," *Proceedings of the IEEE International Conference on Computer Vision*, vol. 2019-Octob, pp. 1314–1324, 2019. https://doi.org/10.1109/ICCV.2019.00140
[32] K. Simonyan and A. Zisserman, "Very deep convolutional networks for large-scale image recognition," *3rd International Conference on Learning Representations, ICLR 2015 - Conference Track Proceedings*, pp. 1–14, 2015.
[33] F. Chollet, "Xception: Deep learning with depthwise separable convolutions," *Proceedings - 30th IEEE Conference on Computer Vision and Pattern Recognition, CVPR 2017*, vol. 2017-Janua, pp. 1800–1807, 2017. https://doi.org/10.1109/CVPR.2017.195
[34] C. Szegedy, V. Vanhoucke, S. Ioffe, J. Shlens, and Z. Wojna, "Rethinking the Inception Architecture for Computer Vision," *Proceedings of the IEEE Computer Society Conference on Computer Vision and Pattern Recognition*, vol. 2016-Decem, pp. 2818–2826, 2016. https://doi.org/10.1109/CVPR.2016.308
[35] K. He, X. Zhang, S. Ren, and J. Sun, "Identity mappings in deep residual networks," *Lecture Notes in Computer Science (including subseries Lecture Notes in Artificial Intelligence and Lecture Notes in Bioinformatics)*, vol. 9908 LNCS, pp. 630–645, 2016. https://doi.org/10.1007/978-3-319-46493-0_38
[36] B. Zoph, V. Vasudevan, J. Shlens, and Q. V. Le, "Learning Transferable Architectures for Scalable Image Recognition," *Proceedings of the IEEE Computer Society Conference on Computer Vision and Pattern Recognition*, pp. 8697–8710, 2018. https://doi.org/10.1109/CVPR.2018.00907
[37] X. Zhang, Z. Li, C. C. Loy, and D. Lin, "PolyNet: A pursuit of structural diversity in very deep networks," *Proceedings - 30th IEEE Conference on Computer Vision and Pattern Recognition, CVPR 2017*, vol. 2017-Janua, no. 1, pp. 3900–3908, 2017. https://doi.org/10.1109/CVPR.2017.415
[38] G. Huang, Z. Liu, L. Van Der Maaten, and K. Q. Weinberger, "Densely connected convolutional networks," *Proceedings - 30th IEEE Conference on Computer Vision and Pattern Recognition, CVPR 2017*, vol. 2017-Janua, pp. 2261–2269, 2017. https://doi.org/10.1109/CVPR.2017.243